Commun Nonlinear Sci Numer Simulat 140 (2025) 108404

Contents lists available at ScienceDirect

Communications in Nonlinear Science and Numerical Simulation

journal homepage: www.elsevier.com/locate/cnsns

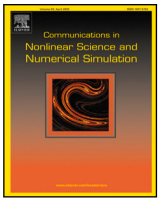

Research paper

Study of immune response in a latent tuberculosis infection model

Hui Cao [a], Jianquan Li [b], Pei Yu [c,*]

[a] School of Mathematics and Data Science, Shaanxi University of Science and Technology, Xi'an, 710021, China
[b] Xi'an Key Laboratory of Human–Machine Integration and Control Technology for Intelligent Rehabilitation, Xijing University, Xi'an, 710123, China
[c] Department of Mathematics, Western University, London, Ontario, N6A 5B7, Canada

ARTICLE INFO

MSC:
92-10
37N25

Keywords:
Mycobacterium tuberculosis
Latent tuberculosis infection
The sustained immune response
Stability
Hopf bifurcation

ABSTRACT

A simple mathematical model describing the immune response during the stage latent tuberculosis infection is established and analyzed. The main purpose of this study is to explore the sustained immune response of the immune system against invaded Mycobacterium tuberculosis in the stage of latent tuberculosis infection. First, the threshold $\mathcal{R}_0$ is defined to determine the occurrence of sustained immune response. Then, stability conditions are derived to show that the sustained immune response may converge to a constant or to a stable periodical oscillation, implying that the Mycobacterium tuberculosis, the infected macrophages, the activated uninfected macrophages, and the immune cells coexist to form the tuberculous granuloma structure. This structure may appear calcified if the system solution converges to a constant, or maintains a dynamic balance if the system solution undergoes a periodical oscillation. These findings well demonstrate the process of sustained immune response in the latent tuberculosis infection as the Mycobacterium tuberculosis is changing. Numerical examples are presented to illustrate the theoretical predictions.

1. Introduction

Tuberculosis (TB) is a chronic respiratory infectious disease due to the infection of human lungs caused by Mycobacterium tuberculosis (Mtb). The Global Tuberculosis Report released by the WHO (World Health Organization) in 2023 [1] estimated that there were 10.6 million TB cases in 2022 in the world, including new cases 133 per 100,000 people. Affected by the COVID-19, the global TB cases and new cases have continued to increase since 2020. The latest research [2] reveals that TB was the leading cause of death arising from a single infectious disease in the world in 2022, and after the COVID-19 epidemic, it has caused nearly twice the number of deaths caused by HIV, reaching a total of 1.13 million deaths. This clearly shows that prevention and control of TB are still an important public health issue that needs to be solved globally.

When the Mtb successfully invades human lungs, the macrophages in the lungs are first activated and then cleared by phagocytosis. However, as the intracellular bacterium, the Mtb may be cleared by the activated macrophages, or may survive to grow or to reproduce within the activated macrophages [3]. If the Mtb is cleared by the activated macrophages that phagocytosed it, TB infection does not occur and the activated macrophages remain uninfected. If the Mtb is not completely eliminated, and survives within the activated macrophages that phagocytosed it, then TB infection occurs, leading to the activated macrophages to be infected. In this case, other immune cells, such as dendritic cells (DCs), B and T cells, neutrophils and so on, will be recruited and join the battle against the Mtb [4]. Eventually, TB granuloma structures are formed by the Mtb, macrophages, and other immune cells in an effort to control the growth of the Mtb. TB granulomas structures generate the environment in which the Mtb may

* Corresponding author.
E-mail address: pyu@uwo.ca (P. Yu).

https://doi.org/10.1016/j.cnsns.2024.108404
Received 15 June 2024; Received in revised form 16 October 2024; Accepted 18 October 2024
Available online 29 October 2024

continue to grow or survive, and may become the battlefield where immune cells kill the Mtb [5]. If TB granuloma can maintain a balance in the immune response, provide enough immune cell activation to inhibit bacterial growth and regulate inflammation, then the infected individuals will be in a state of the latent tuberculosis infection (LTBI). If TB granuloma cannot keep a balance in the immune response, resulting in rapid growth of the number of bacteria, then the LTBI will develop into an active TB [6].

The immune response of an individual after being infected by the Mtb is a complex process, and simple medical experiments have certain limitations. Combining experimental medicine and mathematical modeling enables us to better understand the interaction between the Mtb and the immune system, which provides reasonable explanations for observed phenomena. As early as 1995, in order to study silicosis nodules caused by individuals inhaling quartz particles, Tran et al. [7] used ordinary differential equation (ODE) to establish a mathematical model to describe the clear and phagocytosis of alveolar macrophages after individuals were inhaled quartz particles. Although this model is not directly based on the immune response to lung infection with the Mtb, it still provides a basic dynamical model framework for studying the role of alveolar macrophages in the immune response. Since then, more and more research works have begun to use mathematical models to study the interaction between the immune system and the Mtb, including the ODE models [8–14], the partial differential equation (PDE) models [15–18], the agent-based models [19,20], and the mixed multiscale models [21], etc.

In this paper, based on the interaction between the Mtb and the immune system, we will establish an ODE model to describe the sustained immune response of the immune system against the Mtb. Our purpose is to build a simple model which can characterize the interaction between the immune system and the Mtb in the LTBI stage, and to provide explanation for the process of the persistent immune response of the immune system against the Mtb in the LTBI stage. The rest of the paper is organized as follows. The model formulation and the well-posedness of the system are presented in Section 2. In Section 3, we give an explicit expression of the basic reproduction number $\mathcal{R}_0$, and discuss the existence and stability of the biologically meaningful equilibria. In Section 4, we study the Hopf bifurcation when $\mathcal{R}_0 > 1$ by using normal form theory. In Section 5, numerical simulations are presented to illustrate our theoretical results. Finally, conclusion is given in Section 6.

2. The model and well-posedness

To establish a realistic mathematical model for studying the immune response in a latent tuberculosis infection, we assume that

(i) the macrophages in the host will automatically activate to fight against the invasion of the Mtb;
(ii) no difference exists between the intracellular and extracellular Mtb [22–24], since clinical and epidemiological testing of TB does not separate the Mtb into internal and external parts;
(iii) in order to overcome the difficulty in analysis due to the complexity of immune response process, the difference in the roles of different immune cells, such as DCs, B and T cells, neutrophils as well as other immune cells, in fighting against the Mtb is ignored.

Let $M_U(\tilde{t})$, $M_I(\tilde{t})$, $B(\tilde{t})$, and $T(\tilde{t})$ be the population levels of the activated uninfected macrophages, the infected macrophages, the Mtb, and the immune cells at $\tilde{t}$ time, respectively. Then, a simple ODE model describing the immune response of the immune system against the Mtb is described as follows:

$$\begin{cases} \dfrac{\mathrm{d}M_U}{\mathrm{d}\tilde{t}} = \Lambda_U - \mu_U M_U - \beta B M_U, \\ \dfrac{\mathrm{d}M_I}{\mathrm{d}\tilde{t}} = \beta B M_U - \alpha_T M_I T - \mu_I M_I, \\ \dfrac{\mathrm{d}B}{\mathrm{d}\tilde{t}} = r\mu_I M_I - \gamma_U M_U B - \delta\beta B M_U, \\ \dfrac{\mathrm{d}T}{\mathrm{d}\tilde{t}} = \Lambda_T + \sigma_M M_I T + \sigma_B B T - \mu_T T, \end{cases} \tag{2.1}$$

with the initial conditions,

$$M_U(0) = M_U^0 \geq 0, \quad M_I(0) = M_I^0 \geq 0, \quad B(0) = B^0 \geq 0, \quad T(0) = T^0 \geq 0. \tag{2.2}$$

The definition and typical values of the parameters in system (2.1) are detailed in Table 1.

In system (2.1), we use the bilinear functions $\gamma_U M_U B$, $\beta B M_U$ and $\delta\beta B M_U$ to describe the interaction between activated uninfected macrophages M_U and extracellular Mtb, including clearance, infection and phagocytosis, respectively. Immune cells T eliminate infected macrophages M_I at the rate $\alpha_T M_I T$. Mtb and infected macrophages M_I stimulate the immune system to produce new immune cells T to fight Mtb at the rates $\sigma_B B T$ and $\sigma_M M_I T$, respectively. Infected macrophages M_I undergoes rupture $\mu_I M_I$ due to proliferation of intracellular Mtb, and in this process, the portion $r\mu_I M_I$ in the intracellular Mtb will be released. Activated uninfected macrophages M_U and immune cells T generate new cells at replenishment rates Λ_U and Λ_T, respectively, thereby characterizing immune system of host to be effective even in the absence of Mtb invasion. The natural death rates of activated uninfected macrophages M_U and immune cells T are denoted by μ_U and μ_T, respectively.

To simplify analysis, we introduce the following scaling,

$$M_U = \frac{\mu_U^2}{r\mu_I\sigma_B}x, \quad M_I = \frac{\mu_U^2}{r\mu_I\sigma_B}y, \quad B = \frac{\mu_U}{\sigma_B}z, \quad T = \frac{\mu_U}{\alpha_T}w, \quad \tilde{t} = \frac{t}{\mu_U}.$$

Table 1
Definition and typical values of the parameters in system (2.1).

Parameter	Definition	Value	Unit	Source
α_T	Clearance rate of infected macrophages by immune cells	0.000025	1/day	[22]
γ_U	Clearance rate of Mtb by activated uninfected macrophages	10^{-8}	1/ml/day	[25]
μ_I	Mortality rate of infected macrophages	0.011	1/day	[22]
μ_U	Mortality rate of activated uninfected macrophages	0.0105	1/day	[25]
μ_T	Mortality rate of immune cells	0.1	1/day	[25]
Λ_U	Replenishment rate of activated uninfected macrophages	5000	1/ml/day	[25]
β	Incidence rate of Mtb	10^{-6}	1/day	[25]
r	Average number of Mtb produced by infected macrophage	0.8	1/day	[26]
Λ_T	Natural recruitment of immune cells	10	1/ml/day	[25]
δ	Phagocytosis rate of activated uninfected macrophages	(0, 1)	1/ml/day	[14]
σ_M	Activation rate of immune cells by infected macrophages	0.5	1/day	[25]
σ_B	Activation rate of immune cells by Mtb	0.5	1/day	[25]

into system (2.1) to obtain the dimensionless system,

$$\begin{cases} \dfrac{\mathrm{d}x}{\mathrm{d}t} = C_1 - x - C_2 zx, \\ \dfrac{\mathrm{d}y}{\mathrm{d}t} = C_2 zx - yw - C_3 y, \\ \dfrac{\mathrm{d}z}{\mathrm{d}t} = y - C_4 xz, \\ \dfrac{\mathrm{d}w}{\mathrm{d}t} = C_5 + C_6 yw + zw - C_7 w, \end{cases} \tag{2.3}$$

where the new parameters are defined as

$$C_1 = \frac{r\Lambda_U \mu_I \sigma_B}{\mu_U^3}, \quad C_2 = \frac{\beta}{\sigma_B}, \quad C_3 = \frac{\mu_I}{\mu_U}, \quad C_4 = \frac{\mu_U(\gamma_U + \beta\delta)}{r\mu_I \sigma_B}, \quad C_5 = \frac{\Lambda_T \alpha_T}{\mu_U^2}, \quad C_6 = \frac{\sigma_M \mu_U}{r\mu_I \sigma_B}, \quad C_7 = \frac{\mu_T}{\mu_U}, \tag{2.4}$$

with the following typical values (based on the original parameter values given in Table 1):

$$\begin{aligned} &C_1 = \frac{176000000000}{9261}, \quad C_2 = \frac{1}{500000}, \quad C_3 = \frac{22}{21}, \quad C_4 \in \left(\frac{21}{880000000}, \frac{2121}{880000000}\right), \\ &C_5 = \frac{1000}{441}, \quad C_6 = \frac{105}{88}, \quad C_7 = \frac{200}{21}. \end{aligned} \tag{2.5}$$

In this paper, we will mainly study the dynamic behaviors of system (2.3), and use the obtained theoretical results to explain the process of the sustained immune response of the immune system against the Mtb in the LTBI stage.

First, we consider the nonnegativity and boundedness of solution of system (2.3), and have the following result.

Theorem 2.1. *The solution* $(x(t), y(t), z(t), w(t))$ *of system* (2.3) *starting from any non-negative initial value* $\big(x(0), y(0), z(0), w(0)\big)$ *is non-negative for* $t > 0$*, and ultimately bounded.*

Proof. We first prove the non-negativity, and write the solution of system (2.3) in the form of

$$\begin{aligned} x(t) &= x(0)e^{-\int_0^t (1+C_2 z(s))ds} + C_1 \int_0^t e^{-\int_s^t (1+C_2 z(u))du} ds, \\ y(t) &= y(0)e^{-\int_0^t (C_3+w(s))ds} + C_2 \int_0^t x(s)z(s)e^{-\int_s^t (C_3+w(u))du} ds, \\ z(t) &= z(0)e^{-\int_0^t C_4 x(s)ds} + \int_0^t y(s)e^{-\int_s^t C_4 x(u)du} ds, \\ w(t) &= w(0)e^{-\int_0^t (C_7 - C_6 y(s) - z(s))ds} + C_5 \int_0^t e^{-\int_s^t (C_7 - C_6 y(u) - z(u))du} ds. \end{aligned} \tag{2.6}$$

It is obvious that $x(t) \geq 0$, $t \geq 0$, if $x(0) \geq 0$, and $w(t) \geq 0$, $t \geq 0$, if $w(0) \geq 0$.

Moreover, it can be seen from (2.6) that $y(t)$ and $z(t)$ satisfy that

$$\text{if } y(t) \geq 0, t \geq 0, \text{ then } z(t) \geq 0, t \geq 0; \quad \text{and} \quad \text{if } z(t) \geq 0, t \geq 0, \text{ then } y(t) \geq 0, t \geq 0.$$

We claim that both $y(t) \geq 0$ and $z(t) \geq 0$ are true for $t \geq 0$. Otherwise, without loss of generality, we assume that $y(t)$ crosses zero for the first time at $t = t_1$, and $z(t)$ crosses zero for the first time at $t = t_2$. Then, $y(t_1) = 0$, $y(t) > 0$ for $t < t_1$, and $y(t) < 0$ for $t > t_1$. Similarly, $z(t_2) = 0$, $z(t) > 0$ for $t < t_2$, and $z(t) < 0$ for $t > t_2$. For the case $t_1 \leq t_2$, since $z(t) > 0$ for $t < t_2$, we have

$$y(t_1) = y(0)e^{-\int_0^{t_1} (C_3+w(s))\,ds} + C_2 \int_0^{t_1} x(s)z(s)e^{-\int_s^{t_1} (C_3+w(u))\,du}\, ds > 0, \tag{2.7}$$

which contradicts $y(t_1) = 0$. Therefore, $y(t) \geq 0$ for $t \geq 0$.

Similarly, for the case $t_1 \geq t_2$, we have $y(t) > 0$ for $t < t_1$, and

$$z(t_2) = z(0)e^{-\int_0^{t_2} C_4 x(s)\,ds} + \int_0^{t_2} y(s)e^{-\int_s^{t_2} C_4 x(u)\,du}\,ds > 0. \tag{2.8}$$

This is a contradiction with $z(t_2) = 0$. Hence, $z(t) \geq 0$ for $t \geq 0$.

Having proved the non-negativity, we now turn to prove the boundedness of solution of system (2.3). First, by the expression of $x(t)$ in (2.6), we have

$$\begin{aligned} x(t) &= x(0)e^{-\int_0^t (1+C_2 z(s))\,ds} + C_1 \int_0^t e^{-\int_s^t (1+C_2 z(u))\,du}\,ds \\ &\leq x(0)e^{-t} + C_1 \int_0^t e^{s-t}\,ds \\ &= x(0)e^{-t} + C_1(1 - e^{-t}) \\ &\leq x(0) + C_1, \end{aligned} \tag{2.9}$$

which implies that $x(t)$ is bounded.

Next, we prove that $y(t)$ is bounded. To achieve this, adding the first and second equations in (2.3) yields

$$\begin{aligned} \frac{\mathrm{d}(x+y)}{\mathrm{d}t} &= C_1 - x - yw - C_3 y \\ &\leq C_1 - x - C_3 y \\ &\leq \begin{cases} C_1 - (x+y), & C_3 \geq 1, \\ C_1 - C_3(x+y), & C_3 < 1. \end{cases} \end{aligned} \tag{2.10}$$

Since $x(t) > 0$, $y(t) > 0$ for $t > 0$, the comparison principle implies that

$$x(t) + y(t) \leq \begin{cases} C_1 + (x(0) + y(0) - C_1)e^{-t}, & C_3 \geq 1, \\ \dfrac{C_1}{C_3} + \left(x(0) + y(0) - \dfrac{C_1}{C_3}\right)e^{-C_3 t}, & C_3 < 1, \end{cases} \tag{2.11}$$

which yields $x(t) + y(t) \leq \frac{C_1}{\min\{1, C_3\}} + x(0) + y(0)$ for $t > 0$, and so $y(t) \leq \frac{C_1}{\min\{1, C_3\}} + x(0) + y(0)$ for $t > 0$, implying that $y(t)$ is positive and bounded for $t > 0$.

To prove that $z(t)$ is bounded, we use the argument of contradiction. Suppose otherwise $z(t)$ is unbounded. That is, $z(t) \to +\infty$ as $t \to \infty$. Then, from the first equation of (2.3) we have $\frac{\mathrm{d}x(t)}{\mathrm{d}t} = C_1 - (1 + C_2 z(t))x(t)$ which shows that $x(t) \to 0$ as $t \to \infty$ since $z(t)$ is positive and $z(t) \to +\infty$. This contradicts with that $x(t) > 0$ for $t > 0$. Hence, $z(t)$ is bounded for $t > 0$.

Finally, we prove that $w(t)$ is bounded. We have shown that $x(t)$, $y(t)$ and $z(t)$ are bounded. Similarly, suppose $w(t)$ is unbounded. That is, $w(t) \to +\infty$ as $t \to \infty$. Then, from the second equation of (2.3) we obtain $\frac{\mathrm{d}y(t)}{\mathrm{d}t} = C_2 z(t)x(t) - (C_3 + w(t))y(t)$ which indicates that $y(t) \to 0$ as $t \to \infty$ since $w(t)$ is positive and $w(t) \to +\infty$. This contradicts with that $y(t) > 0$ for $t > 0$. Hence, $w(t)$ is bounded for $t > 0$.

Therefore, the solution $(x(t), y(t), z(t), w(t))$ of system (2.3) is ultimately bounded, and the proof is complete. □

3. Stability and bifurcations of equilibria

In this section, we discuss the dynamic behaviors of system (2.3), including the existence and stability of equilibrium solutions, and possible bifurcations, such as transcritical bifurcation and Hopf bifurcation.

3.1. The existence of equilibrium solutions

In order to discuss the existence of equilibrium solutions of system (2.3), we first use the next generation matrix method [27] to define the basic regeneration number $\mathcal{R}_0$. For this purpose, define

$$\mathcal{F} = \begin{pmatrix} C_2 zx \\ 0 \\ 0 \\ 0 \end{pmatrix}, \quad \mathcal{V} = \begin{pmatrix} yw + C_3 y \\ C_4 xz - y \\ x + C_2 zx - C_1 \\ C_7 w - C_5 - C_6 yw - zw \end{pmatrix}.$$

In the absence of the Mtb, that is, when $z = 0$, we get $x = C_1$, $y = 0$, and $w = \frac{C_5}{C_7}$. Then, using Lemma 1 in [27] we obtain that

$$F = \begin{pmatrix} \frac{\partial \mathcal{F}_1}{\partial y} & \frac{\partial \mathcal{F}_1}{\partial z} \\ \frac{\partial \mathcal{F}_2}{\partial y} & \frac{\partial \mathcal{F}_2}{\partial z} \end{pmatrix} = \begin{pmatrix} 0 & C_1 C_2 \\ 0 & 0 \end{pmatrix}, \quad V = \begin{pmatrix} \frac{\partial \mathcal{V}_1}{\partial y} & \frac{\partial \mathcal{V}_1}{\partial z} \\ \frac{\partial \mathcal{V}_2}{\partial y} & \frac{\partial \mathcal{V}_2}{\partial z} \end{pmatrix} = \begin{pmatrix} C_3 + \frac{C_5}{C_7} & 0 \\ -1 & C_1 C_4 \end{pmatrix},$$

which yields

$$FV^{-1} = \begin{pmatrix} \dfrac{C_2C_7}{C_4(C_5+C_3C_7)} & \dfrac{C_2}{C_4} \\ 0 & 0 \end{pmatrix}.$$

It implies that the basic regeneration number is given by

$$\mathcal{R}_0 = \rho(FV^{-1}) = \frac{C_2C_7}{C_4(C_5+C_3C_7)}.$$

Simply setting $\frac{dx}{dt} = \frac{dy}{dt} = \frac{dz}{dt} = \frac{dw}{dt} = 0$ in system (2.3) yields two equilibrium solutions: a sterile equilibrium solution E_1 and a bacterial equilibrium solution E_2, given as follows:

$$\begin{aligned} E_1 &: \ (x_1, y_1, z_1, w_1) = \left(C_1, 0, 0, \frac{C_5}{C_7}\right), \\ E_2 &: \ (x_2, y_2, z_2, w_2) = \left(\frac{C_1}{1+C_2z_2}, C_4x_2z_2, z_2, \frac{C_2}{C_4} - C_3\right), \end{aligned} \tag{3.1}$$

where z_2 satisfies the following quadratic polynomial equation:

$$\begin{aligned} F(z_2) = {} & C_2(C_2 - C_3C_4)\, z_2^2 + \left\{(1 + C_1C_4C_6)(C_2 - C_3C_4) + C_2\left[C_4(C_5 + C_3C_7) - C_2C_7\right]\right\} z_2 \\ & + C_4(C_5 + C_3C_7) - C_2C_7 = 0. \end{aligned} \tag{3.2}$$

It is clear that E_1 always exists for any feasible parameter values. On the other hand, to have positive equilibrium E_2, it requires that $\frac{C_2}{C_4} - C_3 > 0$, and that $F(z_2)$ has positive real roots. $F(z_2)$ has no positive real roots when $C_4(C_5 + C_3C_7) - C_2C_7 > 0$, and an unique positive real root if $C_4(C_5 + C_3C_7) - C_2C_7 < 0$, yielding $\mathcal{R}_0 > 1$. In addition, $\frac{C_2}{C_4} - C_3 > 0$ implies that $\mathcal{R}_0 = \frac{C_2C_7}{C_4(C_3C_7+C_5)} = \frac{C_2}{C_4C_3+C_4\frac{C_5}{C_7}} < \frac{C_2}{C_4C_3} < 1$.

To understand the biological meaning of the expression $\frac{C_2}{C_4} - C_3 > 0$, we rewrite it in terms of the original parameters as $\frac{\beta r}{\gamma_U+\beta\delta} > 1$. Note that $\frac{1}{\gamma_U+\beta\delta}$ represents the survival period of Mtb, r denotes the average number of Mtb produced by a infected macrophage per unit time, and β is the incidence rate of Mtb. Thus, $\frac{\beta r}{\gamma_U+\beta\delta}$ represents the number of newly infected macrophages during the average survival period of r Mtb, and therefore, $\frac{\beta r}{\gamma_U+\beta\delta} > 1$ implies that the number of newly infected macrophages by r Mtb during their average survival period is greater than 1.

We have the following lemma.

Lemma 3.1. *The polynomial $F(z_2)$ has an unique positive real root when $\mathcal{R}_0 > 1$, and no real roots if $\mathcal{R}_0 < 1$.*

Usually, one solves the polynomial equation $F(z_2) = 0$ for the state variable z_2, and then performs stability analysis. However, for our case, the solution z_2 solved from $F(z_2) = 0$ causes much more difficulty in analyzing the stability of E_2 as well as bifurcating solutions from E_2. To overcome the difficulty, instead of solving $F(z_2) = 0$ for z_2, we solve this equation for C_6 to obtain

$$C_6 = \frac{(1 + C_2z_2)[C_2C_7 - C_4(C_5 + C_3C_7) - (C_2 - C_3C_4)z_2]}{C_1C_4(C_2 - C_3C_4)z_2}. \tag{3.3}$$

It follows from $C_6 > 0$ that

$$C_2C_7 - C_4(C_5 + C_3C_7) - (C_2 - C_3C_4)z_2 = C_4(C_5 + C_3C_7)(\mathcal{R}_0 - 1) - (C_2 - C_3C_4)z_2 > 0, \tag{3.4}$$

yielding $0 < z_2 < \frac{C_4(C_5+C_3C_7)(\mathcal{R}_0-1)}{C_2-C_3C_4} \triangleq z_{max}$. Since $F(z_2)$ is a quadratic polynomial with positive coefficient of z_2^2 and noticing that

$$F(0) < 0 \quad \text{and} \quad F(z_{max}) = C_1C_4^2C_6(C_5 + C_3C_7)(\mathcal{R}_0 - 1) > 0,$$

we know that $F(z_2)$ has an unique positive real root on the interval $(0, z_{max})$ when $C_2 - C_3C_4 > 0$ and $\mathcal{R}_0 > 1$. Summarizing the above results gives the following theorem.

Theorem 3.1. *The system (2.3) always has the sterile equilibrium E_1, and an unique bacterial equilibrium E_2 when $\mathcal{R}_0 > 1$.*

3.2. Stability of the sterile equilibrium E_1

In this subsection, we consider the stability of the sterile equilibrium E_1 and have the following theorem.

Theorem 3.2. *The sterile equilibrium E_1 is globally asymptotically stable (GAS) for $\mathcal{R}_0 < 1$, and unstable for $\mathcal{R}_0 > 1$.*

Proof. The Jacobian matrix of system (2.3) evaluated at the sterile equilibrium E_1 is given by

$$J(E_1)=\begin{pmatrix} -1 & 0 & -C_1C_2 & 0 \\ 0 & -\frac{C_5}{C_7}-C_3 & C_1C_2 & 0 \\ 0 & 1 & -C_1C_4 & 0 \\ 0 & \frac{C_6C_5}{C_7} & \frac{C_5}{C_7} & -C_7 \end{pmatrix},$$

which yields the characteristic polynomial,

$$P_1(\lambda)=(\lambda+1)(\lambda+C_7)\left\{\lambda^2+\frac{1}{C_7}\left[C_5+(C_3+C_1C_4)C_7\right]\lambda+\frac{C_1C_4}{C_7}(C_3C_7+C_5)(1-\mathcal{R}_0)\right\}. \tag{3.5}$$

Obviously, the stability of E_1 is determined by the roots of the quadratic factor in $P_1(\lambda)$, since the other two roots, -1 and $-C_7$, are negative.

Because the two coefficients of the quadratic polynomial factor are positive when $\mathcal{R}_0<1$, the two roots of the quadratic polynomial factor have negative real parts, which implies that E_1 is locally asymptotically stable (LAS) when $\mathcal{R}_0<1$. When $\mathcal{R}_0>1$, E_1 is unstable.

Next, we discuss the global stability of the sterile equilibrium E_1. For this purpose, we construct the function:

$$L(t)=y(t)+\left(C_3+\frac{C_5}{C_7}\right)z(t).$$

Then,

$$\begin{aligned}\frac{\mathrm{d}L(t)}{\mathrm{d}t}&=\frac{\mathrm{d}y(t)}{\mathrm{d}t}+\left(C_3+\frac{C_5}{C_7}\right)\frac{\mathrm{d}z(t)}{\mathrm{d}t}\\&=C_2z(t)x(t)-y(t)w(t)-C_3y(t)+\left(C_3+\frac{C_5}{C_7}\right)\left(y(t)-C_4x(t)z(t)\right)\\&=\left[C_2-C_4\left(C_3+\frac{C_5}{C_7}\right)\right]x(t)z(t)-\left(w(t)-\frac{C_5}{C_7}\right)y(t)\\&=C_2\left(1-\frac{1}{\mathcal{R}_0}\right)x(t)z(t)-\left(w(t)-\frac{C_5}{C_7}\right)y(t).\end{aligned} \tag{3.6}$$

It follows from the 4th equation of (2.3) that $\frac{\mathrm{d}w(t)}{\mathrm{d}t}\geq C_5-C_7w(t)$ due to the non-negativity of solutions. Thus, $w(t)\geq\frac{C_5}{C_7}$ because $w(t)$ is bounded. This yields that $\frac{\mathrm{d}L(t)}{\mathrm{d}t}\leq 0$ when $\mathcal{R}_0<1$. In addition, the non-negativity of the solutions of system (2.3) ensures that $L(t)\geq 0$. By using the pinching principle, we get $\lim_{t\to+\infty}L(t)=0$. This implies that $\lim_{t\to+\infty}(y(t),z(t))=(0,0)$, under which the limit system of system (2.3) is given by

$$\begin{cases}\frac{\mathrm{d}x}{\mathrm{d}t}=C_1-x,\\ \frac{\mathrm{d}w}{\mathrm{d}t}=C_5-C_7w.\end{cases}$$

It is clear that $(x,w)\to(C_1,\frac{C_5}{C_7})$ as t tends to infinity. This shows that E_1 is attractive. Therefore, with E_1 being LAS, the above results imply that the sterile equilibrium E_1 is GAS for $\mathcal{R}_0<1$. □

For the critical case $\mathcal{R}_0=1$, the eigenvalues of $P_1(\lambda)$ become 0, -1, $-C_7$, and $-\frac{C_5}{C_7}-C_1C_4-C_3$. It implies that in the critical case E_1 is a non-hyperbolic equilibrium, and its local stability cannot be determined by linearization. In order to analyze the dynamical behavior of system (2.3) near E_1 at $\mathcal{R}_0=1$, we introduce $x=y_1+C_1$, $y=y_2$, $z=y_3$, and $w=y_4+\frac{C_5}{C_7}$ into (2.3) to obtain

$$\begin{cases}\frac{\mathrm{d}y_1(t)}{\mathrm{d}t}=-y_1-C_2y_1y_3-C_1C_2y_3\triangleq f_1,\\ \frac{\mathrm{d}y_2(t)}{\mathrm{d}t}=-\left(\frac{C_5}{C_7}+C_3\right)y_2+C_1C_2y_3+C_2y_1y_3-y_2y_4\triangleq f_2,\\ \frac{\mathrm{d}y_3(t)}{\mathrm{d}t}=y_2-C_1C_4y_3-C_4y_1y_3\triangleq f_3,\\ \frac{\mathrm{d}y_4(t)}{\mathrm{d}t}=\frac{C_5C_6}{C_7}y_2+\frac{C_5}{C_7}y_3-C_7y_4+C_6y_2y_4+y_3y_4\triangleq f_4.\end{cases} \tag{3.7}$$

Now, $(0,0,0,0)$ is an equilibrium of system (3.7), corresponding to the sterile equilibrium E_1 of system (2.3). The linearized matrix of system (3.7) evaluated at the equilibrium $(0,0,0,0)$ is given by

$$M = \begin{pmatrix} -1 & 0 & -\dfrac{C_1C_4(C_5+C_3C_7)}{C_7} & 0 \\ 0 & -\left(\dfrac{C_5}{C_7}+C_3\right) & \dfrac{C_1C_4(C_5+C_3C_7)}{C_7} & 0 \\ 0 & 1 & -C_1C_4 & 0 \\ 0 & \dfrac{C_5C_6}{C_7} & \dfrac{C_5}{C_7} & -C_7 \end{pmatrix}.$$

Obviously, zero is a simple eigenvalue of M, and the other three eigenvalues of M are -1, $-C_7$, and $-C_1C_4 - C_3 - \frac{C_5}{C_7}$. Next, we project the three stable manifolds onto the center manifold characterized by the zero eigenvalue. To achieve this, we introduce the matrix,

$$Q = \begin{pmatrix} -C_7C_1C_4(C_3C_7+C_5) & 1 & 0 & -\dfrac{C_1C_4(C_3C_7+C_5)}{C_7-C_1C_4C_7-C_3C_7-C_5} \\ C_1C_4C_7^2 & 0 & 0 & -\dfrac{C_5+C_3C_7}{C_7} \\ C_7^2 & 0 & 0 & 1 \\ C_5(1+C_1C_4C_6) & 0 & 1 & \dfrac{(C_5C_7-C_5C_6(C_3C_7+C_5))}{(C_7^3-C_1C_4C_7^2-C_3C_7^2-C_5C_7)} \end{pmatrix},$$

such that $MQ = QA$ with

$$A = \begin{pmatrix} 0 & 0 & 0 & 0 \\ 0 & -1 & 0 & 0 \\ 0 & 0 & -C_7 & 0 \\ 0 & 0 & 0 & -C_1C_4 - C_3 - \frac{C_5}{C_7} \end{pmatrix},$$

and take the linear transformation $(y_1,y_2,y_3,y_4)^T = Q(u_1,u_2,u_3,u_4)^T$. Therefore, the dynamical behavior of system (3.7) near $(0,0,0,0)$ (that is, near E_1 of system (2.3)) at $\mathcal{R}_0 = 1$ is governed by the following 1-d differential equation on the center manifold [28],

$$\frac{\mathrm{d}u_1}{\mathrm{d}t} = \frac{a}{2}u_1^2 + bu_1 + O(u_1^3),$$

where the coefficients a and b can be obtained by using the method and formulas given in [28]. Let ω and v denote the right and left eigenvectors, corresponding to the zero eigenvalue of matrix M, respectively. Standard algebraic manipulations results in

$$\omega = \begin{pmatrix} -\dfrac{C_1C_4(C_5+C_3C_7)}{C_1C_4C_7+C_5+C_3C_7} \\ \dfrac{C_1C_4C_7}{C_1C_4C_7+C_5+C_3C_7} \\ \dfrac{C_7}{C_1C_4C_7+C_5+C_3C_7} \\ \dfrac{C_5}{C_7^2}(1+C_1C_4C_6) \end{pmatrix}, \quad v^T = \begin{pmatrix} 0 \\ 1 \\ \frac{C_5+C_3C_7}{C_7} \\ 0 \end{pmatrix}.$$

Then, the formulas,

$$a = \sum_{k,i,j=1}^{4} v_k\omega_i\omega_j \frac{\partial^2 f_k}{\partial y_i \partial y_j}(0,1), \quad b = \sum_{k,i=1}^{4} v_k\omega_i \frac{\partial^2 f_k}{\partial y_i \partial \mathcal{R}_0}(0,1),$$

given in [28] yield

$$a = -\frac{2C_1C_4C_5(1+C_1C_4C_6)}{C_7(C_1C_4C_7+C_5+C_3C_7)} < 0, \quad b = \frac{C_1C_4(C_5+C_3C_7)}{C_1C_4C_7+C_5+C_3C_7} > 0.$$

Then, Theorem 4 in [28] with $a < 0$ and $b > 0$ ensures the following conclusion.

Theorem 3.3. *The system (2.3) undergoes a forward transcritical bifurcation at $\mathcal{R}_0 = 1$.*

The bifurcation diagram of system (2.3) on the central manifold when $\mathcal{R}_0 = 1$ is shown in Fig. 1, in which the parameter values given in (2.5) have been used. The solid and the dotted lines denote stable and unstable equilibrium solutions, respectively.

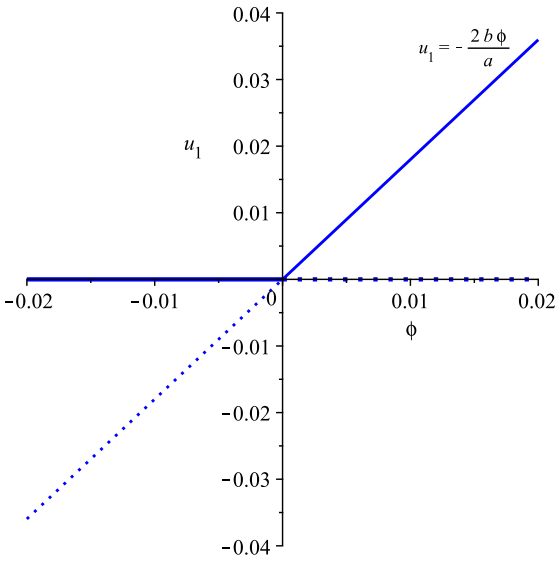

Fig. 1. Bifurcation diagram of system (2.3) on the central manifold when $\mathcal{R}_0 = 1$.

3.3. Stability of the bacterial equilibrium E_2

In order to analyze the stability of the bacterial equilibrium E_2, we first evaluate the Jacobian matrix of system (2.3) at E_2 to obtain

$$J(E_2) = \begin{pmatrix} -(1+C_2z_2) & 0 & -\frac{C_1C_2}{1+C_2z_2} & 0 \\ C_2z_2 & -\frac{C_2}{C_4} & \frac{C_1C_2}{1+C_2z_2} & -\frac{C_1C_4}{1+C_2z_2}z_2 \\ -C_4z_2 & 1 & -\frac{C_1C_4}{1+C_2z_2} & 0 \\ 0 & C_6\left(\frac{C_2}{C_4}-C_3\right) & \frac{C_2}{C_4}-C_3 & \frac{C_1C_4C_6}{1+C_2z_2}z_2+z_2-C_7 \end{pmatrix},$$

which yields the characteristic polynomial,

$$P_2(\lambda) = \lambda^4 + a_1\lambda^3 + a_2\lambda^2 + a_3\lambda + a_4, \tag{3.8}$$

where

$$\begin{aligned}
a_1 &= \frac{1}{C_4(1+C_2z_2)(C_2-C_3C_4)}\Big\{ C_2^2C_4(C_2-C_3C_4)z_2^2 + C_2[(C_2+2C_4)(C_2-C_3C_4)+C_4^2C_5]z_2 \\
&\quad + (C_2+C_4+C_1C_4^2)(C_2-C_3C_4)+C_4^2C_5 \Big\}, \\
a_2 &= \frac{1}{C_4(1+C_2z_2)(C_2-C_3C_4)}\Big\{ (1+C_2z_2)(C_2-C_3C_4)[(C_2-C_3C_4)C_7-C_4C_5-(C_2-C_3C_4)z_2] \\
&\quad + C_2^2[C_4^2C_5+C_2(C_2-C_3C_4)]z_2^2 + C_2[2C_2(C_2-C_3C_4)+C_4C_5(C_2+2C_4)]z_2 \\
&\quad + C_4C_5(C_1C_4^2+C_2+C_4)+(C_2-C_3C_4)(C_1C_4^2+C_2) \Big\}, \\
a_3 &= \frac{1}{C_4(1+C_2z_2)(C_2-C_3C_4)}\Big\{ [(C_2-C_3C_4)C_7-C_4C_5-(C_2-C_3C_4)z_2](C_2-C_3C_4) \\
&\quad [(1+C_2z_2)^2+C_1C_4] + C_4[C_2C_5(1+C_2z_2)^2+C_1C_4^2C_5+C_1(C_2-C_3C_4)^2z_2] \Big\}, \\
a_4 &= \frac{C_1[C_2(C_2-C_3C_4)z_2^2+(C_2-C_3C_4)C_7-C_4C_5]}{1+C_2z_2}.
\end{aligned}$$

It is easy to see that the condition given in (3.4) ensures that a_k $(k = 1, 2, 3) > 0$, and $a_4 > 0$ if $\mathcal{R}_0 > 1$. Therefore, E_2 is LAS if the following two conditions are satisfied:

$$\Delta_2 = a_1a_2 - a_3 > 0, \quad \Delta_3 = a_3\Delta_2 - a_1^2a_4 > 0. \tag{3.9}$$

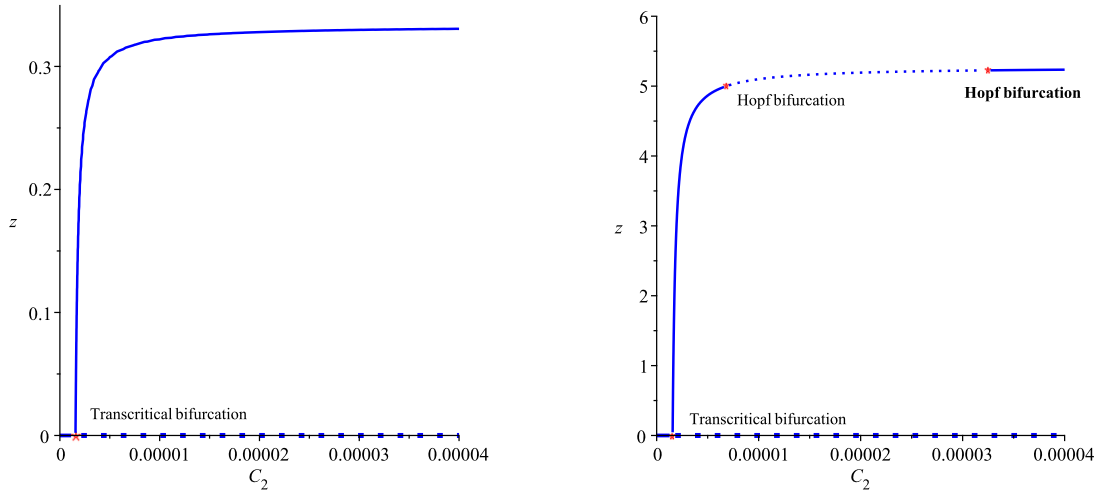

(a) $C_6 = \frac{105}{88}$ (b) $C_6 = 0.0348361$

Fig. 2. Bifurcation diagrams of system (2.3), projected on the C_2-z plane, with two different values of C_6.

We have the following theorem.

Theorem 3.4. *When $C_2 - C_3C_4 > 0$, $\mathcal{R}_0 > 1$, $\Delta_2 > 0$, and $\Delta_3 > 0$, E_2 is LAS.*

Theorem 3.4 implies that if one condition of $\Delta_2 > 0$ and $\Delta_3 > 0$ is not satisfied, E_2 is unstable. It is easy to see that Δ_3 will cross zero before Δ_2 does, indicating that besides the transcritical bifurcation between E_1 and E_2 characterized by $a_4 = 0$ (i.e., $\mathcal{R}_0 = 1$), the only possible bifurcation in system (2.3) from E_2 is Hopf bifurcation, and the system cannot have Bogdanov–Takens (B–T) bifurcation since $a_3 > 0$ when $a_4 = 0$ (see the equations below).

In the following, based on the characteristic polynomial (3.8), we derive the explicit conditions under which the system (2.3) may undergo a transcritical bifurcation or a Hopf bifurcation. First, we consider the transcritical bifurcation. It is known that E_2 exists if and only if $0 < z_2 < z_{max}$, and $C_2 = C_3C_4 + \frac{C_4C_5}{C_7}$ implies that $\mathcal{R}_0 = 1$ and $z_2 = 0$. In addition, when $\mathcal{R}_0 = 1$, we obtain

$$
\begin{aligned}
a_1 &= 1 + C_1C_4 + C_3 + C_7 + \frac{C_5}{C_7} > 0,\\
a_2 &= (1 + C_1C_4 + C_3)C_7 + C_5 + C_3 + C_1C_4 + \frac{C_5}{C_7} > 0,\\
a_3 &= (C_1C_4 + C_3)C_7 + C_5 > 0,\\
a_4 &= 0,\\
\Delta_2 &= (1 + C_7)\Big(C_1C_4 + C_3 + C_7 + \frac{C_5}{C_7}\Big)\Big(1 + C_1C_4 + C_3 + \frac{C_5}{C_7}\Big) > 0,\\
\Delta_3 &= a_3\Delta_2 > 0,
\end{aligned}
$$

showing that the transcritical bifurcation occurs between E_1 and E_2 when $\mathcal{R}_0 = 1$, and the two equilibria E_1 and E_2 actually intersect with the emerging of the bacterial equilibrium E_2.

Next, we consider Hopf bifurcation. Since system (2.3) contains 7 independent free parameters and Hope bifurcation has codimension one, there exist many choices for choosing one bifurcation parameter from the 7 parameters, and treating the other 6 parameters as control parameters. In the following, we choose $C_2 = \frac{\beta}{\sigma_B}$ as the bifurcation parameter because C_2 reflects not only the ability of the Mtb to infect macrophages, but also the ability of the Mtb to stimulate immune cells to produce new immune cells. When C_2 is increased from $C_3C_4 + \frac{C_4C_5}{C_7}$, with z_2 being increased from zero, Δ_3 may cross zero first. It implies that system (2.3) has a Hopf bifurcation emerging at the critical point, $C_2 = C_{2H}$. The bifurcation diagrams are shown in Fig. 2, where C_2 is the bifurcation parameter, and the control parameter C_6 takes two different values, $\frac{105}{88}$ and 0.0348361, with the corresponding bifurcation diagrams given in Fig. 2(a) and (b), respectively. The other parameter values are taken from (2.5).

When $C_6 = \frac{105}{88}$, Fig. 2(a) indicates that system (2.3) can only have a transcritical bifurcation, and Hopf bifurcation is not possible. That is, both $\Delta_2 > 0$ and $\Delta_3 > 0$ are always true regardless of the change in the bifurcation parameter C_2. Obviously, in this case, the variable z, which characterizes the level of the Mtb, is so small that even though TB infection occurs, the infection site will gradually form a TB granulomatous structure. This structure, consisting of the macrophages, the Mtb and the immune cells, appears as a calcified state under the long-term control of the immune system. LTBI does not need to initiate dynamic control to completely

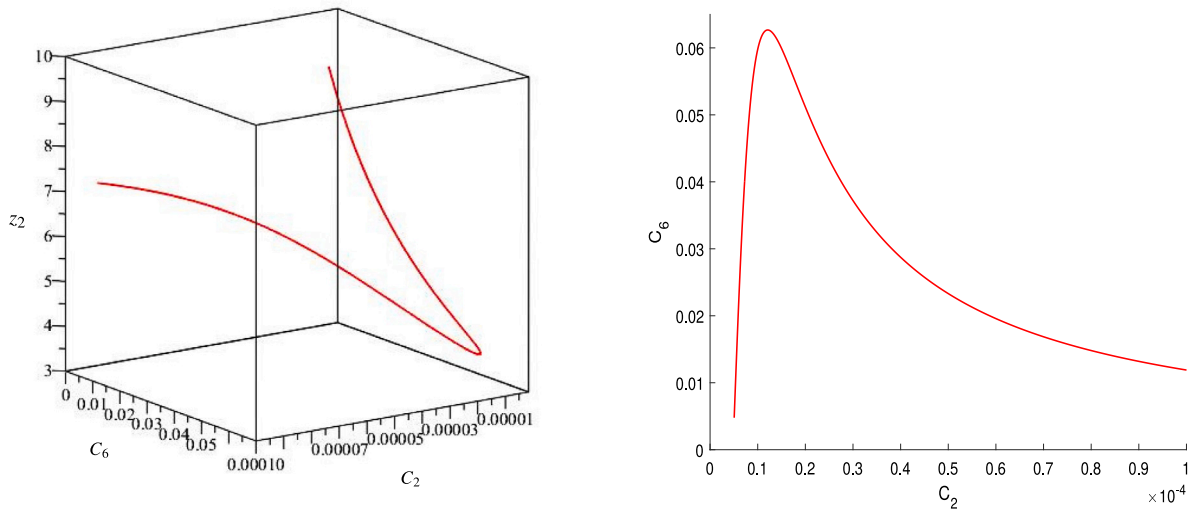

(a) Hopf bifurcation curve in the C_2-C_6-z_2 space

(b) Hopf bifurcation curve projected on the C_2-C_6 plane

Fig. 3. Hopf bifurcation curve of system (2.3) when $\mathcal{R}_0 > 1$.

inhibit the growth and reproduction of the Mtb. In fact, in this case, the Mtb in LTBI will seek every possible opportunity to resist the control of the immune system, yielding its growth and reproduction to increase its numbers. This process of the immune system's continuous fight against the Mtb has to undergo the dynamic control process regardless of the outcome. Therefore, in order to describe the immune response of LTBI when the level of the Mtb increases, we take $C_6 = 0.0348361$ for example, with the bifurcation diagram given in Fig. 2(b). Compared to the values of z in Fig. 2(a), it is obvious that the values of z in Fig. 2(b) have increased significantly, leading to a Hopf bifurcation. This implies that an increase in the Mtb causes the host's immune system to tighten its control, leading to a dynamic confrontation between the Mtb and the immune system, namely, the system (2.3) bifurcates to periodic oscillations.

In the following, we give a detailed analysis on the Hopf bifurcation in system (2.3).

3.4. *Hopf bifurcation from E_2 of system (2.3)*

In this section, we select C_2 and C_6 as the bifurcation parameters to find feasible values for which Hopf bifurcation may occur in system (2.3) when $z_2 \in (0, z_{max})$. Since E_2 exists if and only if $C_2 > C_3C_4 + \frac{C_4C_5}{C_7}$, we take $C_{2c} = C_3C_4 + \frac{C_4C_5}{C_7} = \frac{1377}{88} \times 10^{-7}$. Then, we choose $C_2 \in [C_{2c}, 0.0001]$, $C_6 \in [0, 0.07]$, and $z_2 \in (0, z_{max})$ to display the Hopf bifurcation curve in Fig. 3(a). It is seen that when z_2 approaches 4.0 and continues to increase, the system (2.3) begins to have Hopf bifurcation. To have a better view of the bifurcation, the diagram is projected on the C_2-C_6 plane, as depicted in Fig. 3(b).

According to Fig. 3(a), we fix $z_2 = 5.0$, which is in the range of the Hopf bifurcation, and calculate the particular Hopf critical points. We solve two polynomial equations, $\Delta_3(C_2, C_6) = 0$ and $F(C_2, C_6) = 0$, with the other parameter values given in (2.5) to obtain two Hopf critical points: $(C_{2H_1}, C_{6H_1}) \approx (0.6847069 \times 10^{-5}, 0.0348361)$, and $(C_{2H_2}, C_{6H_2}) \approx (0.000029, 0.0382635)$. Now, as an example, we give a detailed calculation with biological explanation using the bifurcation point (C_{2H_1}, C_{6H_1}) with $z_2 = 5.0$, we get

$$\begin{aligned} &x_2 \approx 1.900378 \times 10^7, \quad y_2 \approx 115.642299, \quad w_2 \approx 4.578354,\\ &a_1 \approx 30.249749, \quad a_2 \approx 61.935488, \quad a_3 \approx 988.719619,\\ &a_4 \approx 956.051454, \quad \Delta_2 \approx 884,813321, \quad \Delta_3 = 4 \times 10^{-994} \approx 0. \end{aligned}$$

Thus, we numerically calculate the Jacobian matrix of system (2.3) at the bacterial equilibrium E_2, and obtain a pure imaginary pair and two negative real eigenvalues: $\pm 5.717099i$, -1.000018 and -29.249730. Therefore, the bacterial equilibrium E_2 is stable for $C_2 \in (C_{2C}, C_{2H_1})$, and loses its stability at $C_2 = C_{2H_1}$, where Hopf bifurcation occurs, leading to a family of bifurcating limit cycles.

In the next section, we apply the method of normal forms to obtain approximate solutions of the bifurcating limit cycles and determine their stability.

4. Normal form computation associated with the Hopf bifurcation

In this section, we pay attention to the Hopf bifurcation determined in the previous section, and apply normal form theory and the Maple program developed in [29,30] to system (2.3) to analyze the Hopf bifurcation which occurs from the bacterial equilibrium

$E_2 = (x_2, y_2, z_2, w_2) = (\frac{C_1}{1+C_2 z_2}, C_4 x_2 z_2, z_2, \frac{C_2}{C_4} - C_3)$ where z_2 satisfies Eq. (3.2) with the bifurcation parameter values at the Hopf critical point $(C_2, C_6) = (C_{2H_1}, C_{6H_1}) \approx (0.6847069 \times 10^{-5}, 0.0348369)$, while other parameter values are given in (2.5).

In order to use the Maple program [29,30], we first apply an affine transformation to system (2.3) so that the linear part of the resulting system is in Jordan canonical form. The affine transformation is given by

$$\begin{pmatrix} x \\ y \\ z \\ w \end{pmatrix} = \begin{pmatrix} \overline{x}(\overline{z}(\mu), \mu) \\ \overline{y}(\overline{z}(\mu), \mu) \\ \overline{z}(\mu) \\ \overline{w}(\overline{z}(\mu), \mu) \end{pmatrix} + P \begin{pmatrix} X_1 \\ X_2 \\ X_3 \\ X_4 \end{pmatrix},$$

where $\mu = C_2 - C_{2H_1}$ is a small perturbation (bifurcation) parameter, and the nonsingular matrix P is obtained by applying the standard eigenvalue–eigenvector method to the Jacobian matrix of system (2.3) at the Hopf critical point as

$$P = \begin{pmatrix} -8.5770458755 & 8.5191977389 & 9999.9594465687 & -4.5648406853 \\ 8.4015606619 & 9.7185327001 & 0.0340385260 & 6.0664497557 \\ 0.4402274367 & 0.3113764245 & -0.0012117211 & -0.9910488092 \\ 0.5670675708 & -0.5377974517 & 0.0002353976 & 0.1241485016 \end{pmatrix},$$

Here, in the affine transformation,

$$\begin{aligned} \overline{x}(\overline{z}(\mu), \mu) &= \frac{C_1}{1 + (C_{2H} + \mu)\overline{z}(\mu)} = \frac{176000000000}{0.06341066765\overline{z} + 9261\overline{z}\mu + 9261}, \\ \overline{y}(\overline{z}(\mu), \mu) &= C_4 \overline{x}(\overline{z}(\mu), \mu)\overline{z}(\mu) = \frac{3400\overline{z}}{0.001006518534\overline{z} + 147\overline{z}\mu + 147}, \\ \overline{w}(\overline{z}(\mu), \mu) &= \frac{C_{2H} + \mu}{C_4} - C_3 = 4.5783539451 + \frac{880000000\mu}{1071}, \end{aligned}$$

with $\overline{z}$ and μ satisfying the following equation, obtained from (3.2):

$$\begin{aligned} G(\overline{z}, \mu) = &\left(3.815228948 \times 10^{-11} + 0.0000124191\mu + \mu^2\right)\overline{z}^2 + \left[\, 0.0000100617 + 1.805733202\mu \right. \\ &\left. + \left(6.847064858 \times 10^{-6} + \mu\right)\left(-0.0000639931 - 9.523809524\mu\right) \,\right] \overline{z} - 0.0000503075 \\ &- 9.523809524\mu \\ = &\, 0. \end{aligned}$$

Substituting the above affine transformation into system (2.3) yields the new system,

$$\frac{\mathrm{d}X_i}{\mathrm{d}t} = H_i(X_1, X_2, X_3, X_4, \mu), \quad i = 1, 2, 3, 4, \tag{4.1}$$

in which

$$\begin{aligned} H_1 = &\, 5.7170987195 X_2 + 3.71207985330 \times 10^6 \mu \\ &+ \left(326830.2043570530 X_1 - 231172.4944986856 X_2 + 1053.7289429942 X_3 \right. \\ &\left. - 735771.3553032691 X_4\right)\mu + o(\mu) \\ &+ 0.1922718318 X_1^2 - 0.0620896095 X_1 X_2 - 0.0014023895 X_1 X_3 - 0.4948630759 X_1 X_4 \\ &- 0.1140505404 X_2^2 + 0.0002722396 X_2 X_3 + 0.5355698656 X_2 X_4 \\ &+ 1.6487098386 \times 10^{-6} X_3^2 + 0.0012181016 X_3 X_4 - 0.1175569095 X_4^2, \\ H_2 = &- 5.7170987195 X_1 + 4.6306136881 \times 10^6 \mu \\ &+ \left(407702.5489213164 X_1 + 288374.8625162197 X_2 + 1314.4684004223 X_3 \right. \\ &\left. - 917833.9485805878 X_4\right)\mu + o(\mu) \\ &- 0.5933801127 X_1^2 - 0.0261310320 X_1 X_2 - 0.0007202012 X_1 X_3 + 0.0867158769 X_1 X_4 \\ &+ 0.5584867386 X_2^2 + 0.0009566335 X_2 X_3 - 0.3343683318 X_2 X_4 \\ &- 1.63477219747788 \times 10^{-6} X_3^2 - 0.0011352446 X_3 X_4 + 0.0474261651 X_4^2, \\ H_3 = &- 1.0000184683 X_3 - 8846.1246339803 \mu \\ &- \left(778.8573619508 X_1 + 550.8988974108 X_2 + 2.5111037285 X_3 \right. \\ &\left. - 1753.3903817666 X_4\right)\mu + o(\mu) \\ &+ 0.0006243108 X_1^2 - 0.0000473311 X_1 X_2 - 1.5233847387 \times 10^{-6} X_1 X_3 \\ &- 0.0005862315 X_1 X_4 - 0.0005166366 X_2^2 - 7.7557014660 \times 10^{-7} X_2 X_3 \\ &+ 0.0008048624 X_2 X_4 + 4.4107297386 \times 10^{-9} X_3^2 + 3.32624899993 \times 10^{-6} X_3 X_4 \\ &- 0.0001582688 X_4^2, \end{aligned}$$

$$
\begin{aligned}
H_4 = &-29.2497300817X_4 + 3.1038169085\times 10^6\mu \\
&+ \big(273275.6714771630X_1 + 193292.4736422569X_2 + 881.0644812286X_3 \\
&- 615207.5557695441X_4\big)\mu + o(\mu) \\
&- 0.1010309413X_1^2 - 0.0357891208X_1X_2 + 0.0045569267X_1X_3 \\
&- 0.1925661099X_1X_4 + 0.1248125017X_2^2 + 0.0042452865X_2X_3 + 0.1328341770X_2X_4 \\
&- 0.0000146616X_3^2 - 0.0119859985X_3X_4 - 0.0373126825X_4^2,
\end{aligned}
$$

with $o(\mu)$ representing higher-order terms of μ.

Now, the Jacobian matrix of system (4.1) evaluated at the equilibrium, $X_i = 0$ $(i = 1,2,3,4)$ and the critical point, $\mu = 0$ (corresponding to the bacterial equilibrium E_2 of the system (2.3)) is in the Jordan canonical form:

$$
J_1(0) = \begin{pmatrix} 0 & 5.717098720 & 0 & 0 \\ -5.717098720 & 0 & 0 & 0 \\ 0 & 0 & -1.000018468 & 0 \\ 0 & 0 & 0 & -29.24973008 \end{pmatrix}.
$$

Applying the formula (18) in [31] to system (2.3) yields

$$
\begin{aligned}
v_0 &= \frac{1}{2}\Big(\frac{\partial^2 H_1}{\partial X_1\partial\mu} + \frac{\partial^2 H_2}{\partial X_2\partial\mu}\Big)\Big|_{X_i=0,\,\mu=0} \approx 307602.5334366363, \\
\tau_0 &= \frac{1}{2}\Big(\frac{\partial^2 H_1}{\partial X_2\partial\mu} - \frac{\partial^2 H_2}{\partial X_1\partial\mu}\Big)\Big|_{X_i=0,\,\mu=0} \approx -88265.0272113154.
\end{aligned} \tag{4.2}
$$

Next, substituting $\mu = 0$ into (4.1), and then applying the Maple program [29], we obtain

$$
v_1 = -0.3467351308\times 10^{-3}, \quad \tau_1 = -0.2029977230\times 10^{-2}. \tag{4.3}
$$

Therefore, the normal form associated with this Hopf bifurcation, up to third-order terms, is given by

$$
\begin{aligned}
\dot r &= r\,(v_0\mu + v_1 r^2) \\
&= r\,(307602.5334366363\mu - 0.3467351308\times 10^{-3} r^2), \\
\dot\theta &= \omega_c + \tau_0\mu + \tau_1 r^2 \\
&= 5.717098720 - 88265.0272113154\mu - 0.2029977230\times 10^{-2} r^2.
\end{aligned} \tag{4.4}
$$

The steady-state solutions of Eq. (4.4) are determined from $\dot r = \dot\theta = 0$, resulting in

$$
\bar r = 0, \quad \bar r^2 = 8.871397966\times 10^8\mu. \tag{4.5}
$$

The equilibrium $\bar r = 0$ represents the bacterial equilibrium solution E_2 of the system (2.3). A linear analysis on the first differential equation of (4.4) shows that $\frac{\mathrm{d}}{\mathrm{d}r}(\frac{\mathrm{d}r}{\mathrm{d}t})|_{\bar r=0} = v_0\mu$, and thus $\bar r = 0$ (E_2) is LAS (unstable) for $\mu < 0$ (> 0), as expected. When μ is increased from negative to cross zero, Hopf bifurcation occurs and the amplitude of the bifurcating limit cycle is approximated by the nonzero steady state solution,

$$
\bar r \approx 29784.89209\sqrt{\mu}. \tag{4.6}
$$

Since $\frac{\mathrm{d}}{\mathrm{d}r}(\frac{\mathrm{d}r}{\mathrm{d}t})|_{(4.6)} = 2v_1\mu < 0$ $(\mu > 0,\ v_1 < 0)$, the Hopf bifurcation is supercritical since $v_1 < 0$ and so the bifurcating limit cycle is stable.

Similarly, we can analyze the Hopf bifurcation around the bacterial equilibrium E_2 at the critical point $(C_{2H_2}, C_{6H_2}) \approx (0.000029, 0.0382635)$ using the above procedure. The detailed analysis for this part is omitted for simplicity.

5. Numerical simulation

The theoretical results obtained in the previous section show that when the bacterial threshold $\mathcal{R}_0 < 1$, the sterile equilibrium E_1 of the model is GAS; as $\mathcal{R}_0$ is increased to cross 1, the system has an unique bacterial equilibrium E_2, which is LAS within the interval $C_2 \in (C_{2C}, C_{2H_1})$ or $(C_{2H_2}, +\infty)$, and bifurcates to periodic oscillations for $C_2 \in [C_{2H_1}, C_{2H_2}]$.

In this section, numerical simulations are presented to compare with the analytical predictions, in particular, for the Hopf bifurcation. In order to give a good comparison, we take the parameter values from (2.5), but treat C_2 as the bifurcation parameter, which is varied to show the stable equilibria E_1 and E_2, as well as stable limit cycles bifurcating from E_2.

First, we demonstrate the dynamic behaviors of system (2.3) for $C_2 \in [0, 0.00005]$ in Fig. 4, with respect to the activated uninfected macrophages, the infected macrophages, the Mtb, and the immune cells as the parameter C_2 is varied. Taking Fig. 4(c) as an example, when $C_2 \in [0, C_{2c})$, the infected macrophages is zero, which means that the sterile equilibrium E_1 is GAS; when $C_2 \in (C_{2c}, C_{2H_1})$, the infected macrophages keep the constant, which implies that the bacterial equilibrium E_2 is LAS; when $C_2 \in [C_{2H_1}, C_{2H_2}]$, the infected macrophages experiences periodic oscillations due to Hopf bifurcation; when $C_2 \in (C_{2H_2}, +\infty)$, the periodic oscillation of the infected macrophages stops, and returns to the equilibrium E_2 again.

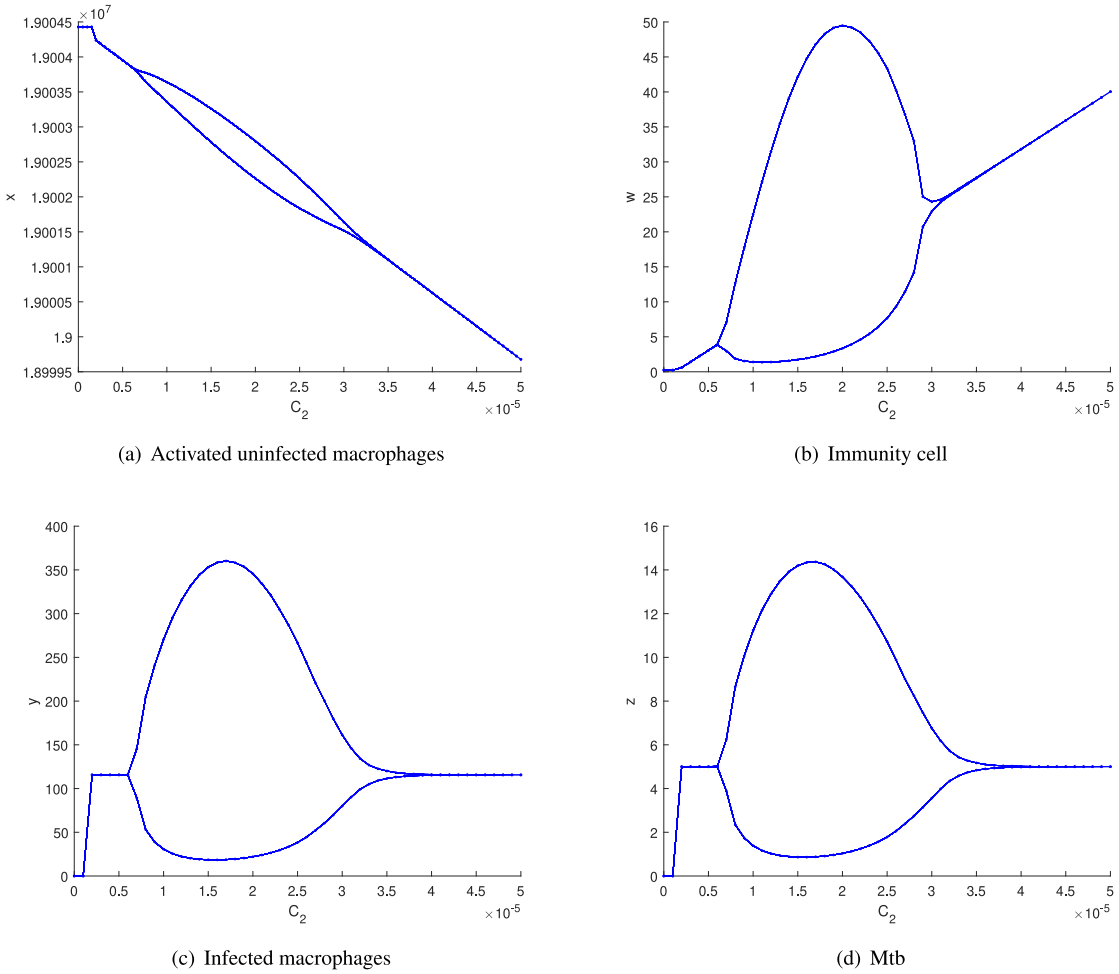

(a) Activated uninfected macrophages (b) Immunity cell

(c) Infected macrophages (d) Mtb

Fig. 4. Bifurcation diagrams of system (2.3) at $z_2 = 5$.

Next, we give a detailed analysis on the dynamic behaviors of the system (2.3) for different values of C_2 in the interval $C_2 \in [0, 0.00005]$ and show the corresponding biological significance. When we take $C_2 = 0.1 \times 10^{-5} \in [0, C_{2c})$, as shown in Fig. 5, all three different solutions of system (2.3) with three different initial values converge to the sterile equilibrium E_1. The simulation results indicate that E_1 is stable, consistent with Theorem 3.2, implying that when $C_2 < C_{2C}$, although the Mtb has entered the lungs of the host, the immune system of the host completely eliminates the invading Mtb, and TB infection does not occur.

When we choose $C_2 = 0.345 \times 10^{-5} \in (C_{2C}, C_{2H_1})$, yielding that $C_2 - C_3C_4 > 0$, $\mathcal{R}_0 > 1$, $\Delta_2 > 0$, and $\Delta_3 > 0$. In this case, system (2.3) has a stable focus, see Fig. 6(a), which is consistent with Theorem 3.4. The results indicate that when $C_2 \in (C_{2C}, C_{2H_1})$, the immune system of host cannot completely eliminate the invading Mtb, and Mtb will survive in the lungs of host. That is, TB infection occurs, which implies that the host first enters the stage of LTBI. In this stage, the immune system initiates the sustained immune response to control the reproduction and growth of the Mtb that survive in the lungs of host, and the infection will eventually develop into calcification.

As the bifurcation parameter C_2 increases and enters the interval $[C_{2H_1}, C_{2H_2}]$, the bacterial equilibrium E_2 is no longer stable, and system (2.3) experiences periodical oscillations, due to Hopf bifurcation, see Fig. 7. Here, the same initial value is taken for simulations, displaying 3-d phase portraits for the infected macrophages, the Mtb, and the immune cells at different values of C_2. This situation means that the host's immune function is getting weak, causing the Mtb dormant inside the calcified area to revive and begin to grow and multiply. Accordingly, the immune system will recruit more activated macrophages and T cells to the infection site to fight and control the Mtb. Then, the immune system of host and the Mtb will begin a mutual restraint mode as one is increasing while the other is decreasing, that is, the system (2.3) shows periodic oscillations. Taking Fig. 7(a) as an example, it is seen that the infected macrophages increase as the Mtb in the lungs increases. Correspondingly, the immune system will recruit more immune T cells to control the growth and reproduction of the Mtb in the lungs. Once the Mtb is controlled by the immune system and begins to decrease, the level of infected macrophages and immune T cells will decrease accordingly. It shows that the immune system of host dynamically controls the invading Mtb, and the immune system and the Mtb enter a dynamic counterbalancing stage. Of course, the host is still in the state of LTBI.

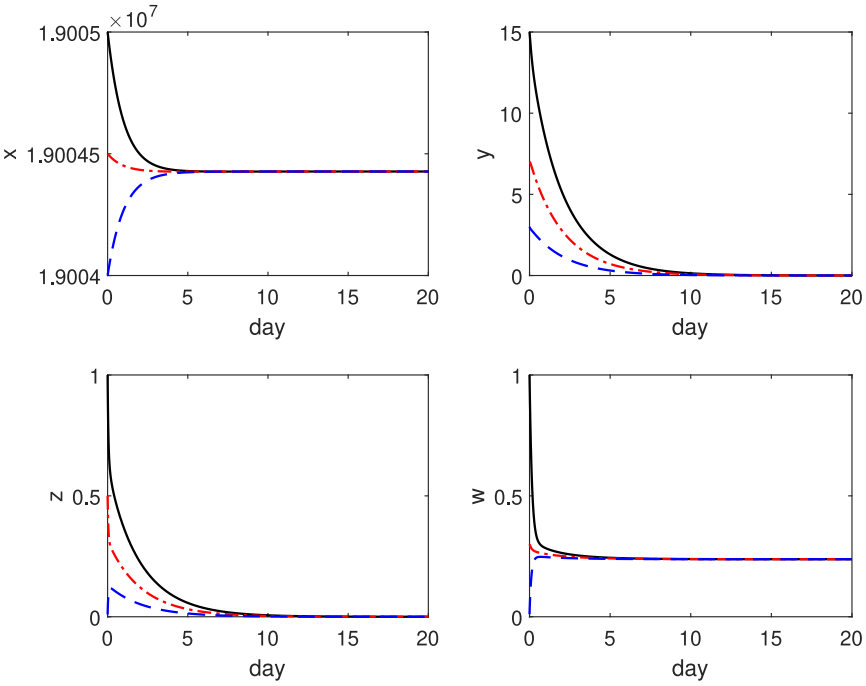

Fig. 5. The stability of E_1 of system (2.3) for $C_2 = 0.1 \times 10^{-5} \in (0, C_{2c})$ $(0 < \mathcal{R}_0 < 1)$.

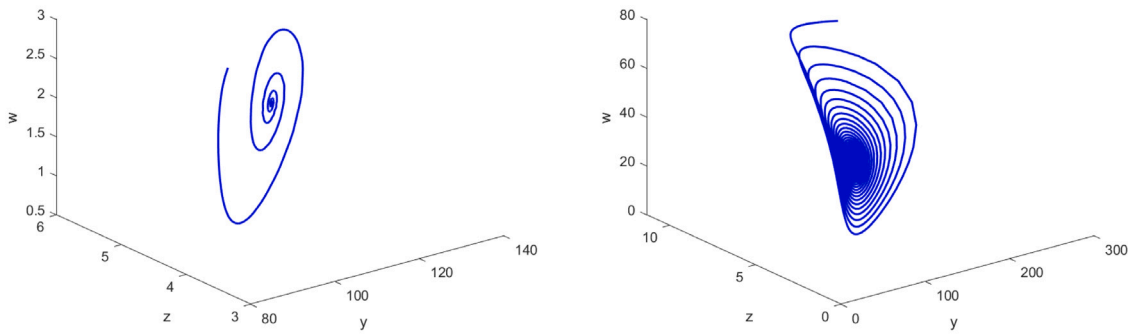

(a) $C_2 = 0.345 \times 10^{-5}$ (b) $C_2 = 0.00004$

Fig. 6. Stable E_2 of system (2.3) when (a) $C_{2C} < C_2 < C_{2H_1}$; and (b) $C_2 > C_{2H_2}$.

As C_2 continues to increase, we choose $C_2 = 0.00004 > C_{2H_2} = 0.000029$, yielding $C_2 - C_3C_4 > 0$, $\mathcal{R}_0 > 1$, $\Delta_2 > 0$, and $\Delta_3 > 0$. Then, system (2.3) has a stable focus, as shown in Fig. 6(b), which agrees with Theorem 3.4. It implies that when $C_{2C} > C_{2H_2}$, as the ability of immune system to fight the Mtb increases, the Mtb is completely controlled and loses the ability to continue growing and reproducing. It also means that the dynamic balance between the immune system and the Mtb ends, and the infection site will calcify again over time. Of course, the Mtb enters a dormant state again, and the host remains LTBI.

6. Conclusion and discussion

In this paper, based on the process of the immune system fighting against the Mtb during the stage of LTBI, we have successfully built a simple mathematical model to analyze the sustained immune response of the system. Our theoretical analysis reveals that the dynamic behaviors of the system changes as a bifurcation parameter (C_2) is varied. In fact, it follows from $C_2 = \frac{\beta}{\sigma_B}$ that either an increase in the incidence rate β of the activated uninfected macrophages becoming the infected macrophages, or a decrease in the activation rate σ_B of the immune cells by the Mtb, will lead to an increase in the parameter C_2. Furthermore, it is seen that when the Mtb invades the host's lungs, the immune system may clear the invading Mtb and TB infection will not occur, which corresponds to the stable sterile equilibrium E_1 of system (2.3); however, when the ability of the Mtb to infect the activated uninfected macrophages

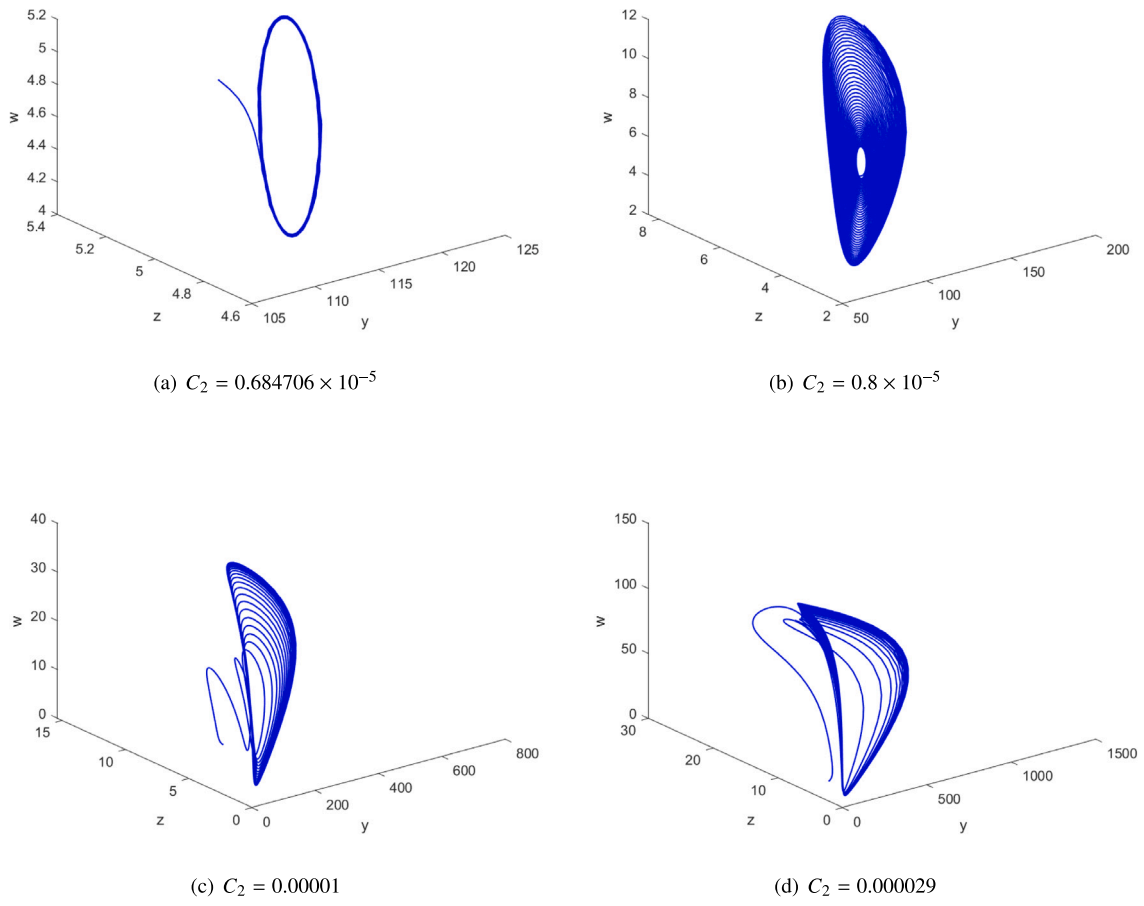

(a) $C_2 = 0.684706 \times 10^{-5}$ (b) $C_2 = 0.8 \times 10^{-5}$

(c) $C_2 = 0.00001$ (d) $C_2 = 0.000029$

Fig. 7. Hopf bifurcations in system (2.3) for $C_2 \in [C_{2H_1}, C_{2H_2}]$.

is enhanced, the immune system may no longer be able to completely remove the invading Mtb and TB infection occurs, implying that the host enters the stage of LTBI, which corresponds to the dynamic behaviors of the system (2.3) for $\mathcal{R}_0 > 1$. During the stage of LTBI, the immune system will initiate the sustained immune response to control the growth and reproduction of the Mtb in the lungs, and TB granulomas are formed accordingly.

TB granuloma is a structure composed of the macrophages, the Mtb and some other immune cells during the host's sustained immune response in which the immune system fights against the Mtb. It is the environment in which the Mtb may survive, grow and even multiply, and also be the battlefield where the immune cells kill the Mtb. When the Mtb simply survives within the structure of a TB granuloma, it implies that the number and virulence of the Mtb are limited and the immune system can control its development and eventually calcify it. When the Mtb only survives within TB granulomatous structures, it implies that the Mtb has a limited ability to infect the activated uninfected macrophages, allowing the immune system to control its development and eventual calcification, which corresponds to the stable bacterial equilibrium E_2 of system (2.3). And if the ability of the Mtb to infect the activated uninfected macrophages increases, the calcified structure may revive again. In this case, the immune system will start a dynamic fight against the Mtb, which corresponds to system (2.3) which generates periodic oscillations. During this stage, the immune system control becomes strong as the Mtb is more infective, and becomes weak as the Mtb is less infective. As the Mtb continues to increase its infectivity, the immune system will also increase its ability to control the Mtb, and becomes so strong that it ultimately stops the control, causing its calcification.

As a matter of fact, there are two possibilities for ending the dynamic control process. One is that the immune system wins, the Mtb is controlled, and the TB granulomas formed at the infection site will gradually calcify; the other is that the Mtb wins, the immune system cannot independently control the Mtb, and the host will develop from a LTBI to an activate TB. In this paper, we have studied the first case, and left the second case for future work.

CRediT authorship contribution statement

Hui Cao: Writing – review & editing, Writing – original draft, Validation, Investigation, Formal analysis, Conceptualization. **Jianquan Li:** Writing – original draft, Validation, Software, Investigation, Formal analysis. **Pei Yu:** Writing – review & editing, Writing – original draft, Validation, Supervision, Software, Methodology, Formal analysis.

Declaration of competing interest

The authors declare that they have no known competing financial interests or personal relationships that could have appeared to influence the work reported in this paper.

Acknowledgments

This work was supported by the National Natural Science Foundation of China (Grant Nos. 12071268, 11971281), the Innovation Capability Support Program of Shaanxi Province (No. 2023-CX-TD-61), and the Natural Sciences and Engineering Research Council of Canada, Canada (No. R2686A02).

Data availability

No data was used for the research described in the article.

References

[1] Global tuberculosis report 2023. World Health Organization, https://www.who.int/tb/publications/global_report/en/.
[2] Millington KA, White RG, Lipman M, et al. The 2023 UN high-level meeting on tuberculosis: renewing hope, momentum, and commitment to end tuberculosis. Lancet Respir Med 2024;12(1):10–3. http://dx.doi.org/10.1016/S2213-2600(23)00409-5.
[3] Ernst JD. The immunological life cycle of tuberculosis. Nat Rev Immunol 2012;12:581–91. http://dx.doi.org/10.1038/nri3259.
[4] Ramakrishnan L. Revisiting the role of the granuloma in tuberculosis. Nat Rev Immunol 2012;12:352–66. http://dx.doi.org/10.1038/nri3211.
[5] Davis JM, Ramakrishnan L. The role of the granuloma in expansion and dissemination of early tuberculous infection. Cell 2009;136:37–49. http://dx.doi.org/10.1016/j.cell.2008.11.014.
[6] Flynn JL, Chan J, Lin PL. Macrophages and control of granulomatous inflammation in tuberculosis. Immunology 2011;4(3):271–8. http://dx.doi.org/10.1038/mi.2011.14.
[7] Tran CL, Jones AD, Donaldson K. Mathematical model of phagocytosis and inflammation after the inhalation of quartz at different concentrations. Scand J Work Environ Health 1995;21(2):50–4, PMID: 8929690.
[8] Wigginton J, Kirschner D. A model to predict cell-mediated immune regulatory mechanisms during human infection with Mycobacterium tuberculosis. J Immunol 2001;166:1951–67. http://dx.doi.org/10.4049/jimmunol.166.3.1951.
[9] Gammack D, Ganguli S, Marino S, et al. Understanding the immune response in tuberculosis using different mathematical models and biological scales. Multiscale Model Simul 2005;3(2):312–45. http://dx.doi.org/10.1137/040603127.
[10] Magombedze G, Garira W, Mwenje E. Modelling the human immune response mechanisms to mycobacterium tuberculosis infection in the lungs. Math Biosci Eng 2006;3(4):661–82. http://dx.doi.org/10.3934/mbe.2006.3.661.
[11] Day J, Friedman A, Schlesinger LS. Modeling the immune rheostat of macrophages in the lung in response to infection. Proc Natl Acad Sci 2009;106:11246–51. http://dx.doi.org/10.1073/pnas.0904846106.
[12] Garira W, Mathebula D, Netshikweta R. A mathematical modelling framework for linked within-host and between-host dynamics for infections with free-living pathogens in the environment. Math Biosci 2014;256:58–78. http://dx.doi.org/10.1016/j.mbs.2014.08.004.
[13] Kwasi-Do Ohene Opoku N, Mazandu GK. Modelling the human immune response dynamics during progression from Mycobacterium latent infection to disease. Appl Math Model 2020;80:217–37. http://dx.doi.org/10.1016/j.apm.2019.11.013.
[14] Zhang W. Analysis of an in-host tuberculosis model for disease control. Appl Math Lett 2020;99:105983. http://dx.doi.org/10.1016/j.aml.2019.07.014.
[15] Hao W, Crouserb ED, Friedmanc A. Mathematical model of sarcoidosis. Proc Natl Acad Sci 2014;111(45):16065–70. http://dx.doi.org/10.1073/pnas.1417789111.
[16] Hao W, Schlesinger LS, Friedman S. Modeling granulomas in response to infection in the lung. PLoS One 2016;11(3):e0148738. http://dx.doi.org/10.1371/journal.pone.0148738.
[17] S. Marino S, El-Kebir M, Kirschner D. A hybrid multi-compartment model of granuloma formation and T cell priming in tuberculosis. J Theoret Biol 2011;280:50–62. http://dx.doi.org/10.1016/j.jtbi.2011.03.022.
[18] Fallahi-Sichani M, Schaller NA, Kirschner DE, et al. Identification of key processes that control tumor necrosis factor availability in a tuberculosis granuloma. PLoS Comput Biol 2010;6(5):e1000778. http://dx.doi.org/10.1371/journal.pcbi.1000778.
[19] Segovia-Juarez JI, Ganguli S, Kirschner D. Identifying control mechanisms of granuloma formation during m. tuberculosis infection using an agent-based model. J Theoret Biol 2004;231:357–76. http://dx.doi.org/10.1016/j.jtbi.2004.06.031.
[20] Ray JC, Flynn JL, Kirschner DE. Synergy between individual TNF-dependent functions determines granuloma performance for controlling Mycobacterium tuberculosis infection. J Immunol 2009;182:3706–17. http://dx.doi.org/10.4049/jimmunol.0802297.
[21] Kirschner D, Pienaar E, Marino S, et al. A review of computational and mathematical modeling contributions to our understanding of Mycobacterium tuberculosis within-host infection and treatment. Curr Opin Syst Biol 2017;170–85. http://dx.doi.org/10.1016/j.coisb.2017.05.014.
[22] Ibarguen-Mondragon E, Esteva L, Chavez-Galan. A mathematical model for cellular immunology of tuberculosis. Math Biosci Eng 2011;8(4):973–86. http://dx.doi.org/10.3934/mbe.2011.8.973.
[23] Ibarguen-Mondragon E, Esteva L, Burbano-Rosero EM. Mathematical model for the growth of mycobacteriun tuberculosis in the granuloma. Math Biosci Eng 2018;15(2):407–28. http://dx.doi.org/10.3934/mbe.2018018.
[24] Jin Y, Cao H, Xu X. Analysis of a simple mathematical model describing tuberculous granuloma. Int J Math Sci Eng Appl 2023;4(4):249–63. http://dx.doi.org/10.5206/mase/16678.
[25] Du Y, Wu J, Heffernan JM. A simple in-host model for Mycobacterium tuberculosis that captures all infection outcomes. Math Popul Stud 2017;24(1):37–63. http://dx.doi.org/10.1080/08898480.2015.1054220.

[26] Sud D, Bigbee C, Flynn JAL, et al. Contribution of CD8+ T cells to control of Mycobacterium tuberculosis infection. J Immunol 2006;176(7):4296–314. http://dx.doi.org/10.4049/jimmunol.176.7.4296.
[27] Van den Driessche P, Watmough J. Reproduction numbers and sub-threshold endemic equilibria for compartmental models of disease transmission. Math Biosci 2002;180:29–48. http://dx.doi.org/10.1016/s0025-5564(02)00108-6.
[28] Castillo-Chavez C, Song B. Dynamical models of tuberculosis and their applications. Math Biosci Eng 2004;1:361–404. http://dx.doi.org/10.3934/mbe.2004.1.361.
[29] Yu P. Computation of normal forms via a pertubation technique. J Sound Vib 1998;211:19–38. http://dx.doi.org/10.1006/jsvi.1997.1347.
[30] Yu P. A simple and efficient method for computation center manifold and normal forms associated with semi-simple cases. Dyn Contin Discrete Impuls Syst Ser B Appl Algorithms 2003;10:273–86, https://api.semanticscholar.org/CorpusID:122602005.
[31] Zhang WJ, Yu P. Hopf and generalized Hopf bifurcations in a recurrent autoimmune disease model. Int J Bifurcation Chaos 2016;26(5):1650079. http://dx.doi.org/10.1142/S0218127416500796.